Population Characteristics of *Balanophyllia elegans* in the San Juan Archipelago

Hana Dubail

University of Washington

ABSTRACT: Determining predictors of *Balanophyllia elegans'* population distribution and physical size is important for ecological research in the Eastern Pacific because changes in this species' biomass, abundance, and environment could be an indication of realized impact from climate change and ocean acidification. Over the last four decades community composition has changed around the San Juan Islands, including a decline in *B. elegans'* density. In this study we assessed abundance, biomass, population density, largest diameter, and surface area at 11 sites from the years 2008-2013, at depths ranging from 3 m to 27.5 m with 3 m increments, and at four flow ranks, looking for patterns and predictors. We found that all three variables (site, year, and depth) and the interaction variables 'site + depth' and 'site + year + depth' are statistically significant predictors for coral distribution, and year, depth, and the interaction term 'year + site' are significant predictors for oral disc surface area. These results tell us that these sites are unique, but each site has an interesting pattern that will need to be defined through further analysis for a larger sample size.

INTRODUCTION

Climate change is causing a global ocean trend towards warmer surface temperatures and decreased pH (Orr et al. 2005). It is important to determine how this is changing ocean ecology for conservation efforts and future predictions of ocean processes, because the ocean's ability to provide services and commodities to a growing human population is decreasing. Consequences of the increasing rate of greenhouse gas released into the atmosphere are still largely unknown. The buffering quality of the ocean is partially responsible for our uncertainty because it is estimated that half of the CO_2 released from industry, the burning of fossil fuels, and land use practices is absorbed by the ocean (Maier-Reimer and Hasselmann 1987). Dissolved CO_2 reacts with carbonate ions and water, which decreases the carbonate concentration and impedes calcifying organisms' ability to construct their calcium carbonate ($CaCO_3$) skeletons (Orr 2005). Orr et al. (2005) estimate that surface carbonate concentrations have already declined more than 10% compared to pre-industrialization. Although this means that the air is cleaner than it would be without the ocean's carbon sink, the effects of climate change are delayed and spread through larger ecosystems.

Balanophyllia elegans, commonly called the orange cup coral*,* is a scleractinian (hard skeleton), solitary coral that builds a $CaCO_3$ skeleton (Altieri 2003). Along the western coast of North America, in the eastern Pacific, *B. elegans* is found in intertidal and subtidal areas down to ~587 m depth from Vancouver, Canada to Baja California, Mexico (Fadlallah 1983). They are on average 10 mm in diameter and are found primarily on vertical rock walls (Bruno 1996 and Chadwick 1991). The 2000 km range of *B. elegans* is much larger than would be expected given

their dispersal ability since the *B. elegans* planula larvae have not been observed swimming or moving by means other than crawling (Gerrodette 1981). In laboratory studies, the planulae traveled 130 cm over 3 days on average before settling (Gerrodette 1981). Under these conditions, *B. elegans* would extend its range by only 7.5 cm/yr. In California studies, these cup corals were estimated to live between 6-40 yrs (Bruno 1996). Gerrodette (1981) postulates that there must be chance events that are spreading the coral further than they are inherently capable of doing by crawling.

At many sites around the San Juan Islands, Washington, *Balanophyllia elegans* is abundant, but its population may be decreasing. Elahi et al. (2013) found that community composition has changed over the last four at research locations around the San Juan Islands, perhaps in response to increased water temperature and acidity. The results from this study showed an increase in sessile richness and diversity in the modern quadrats. However, with the introduction of new species, there were decreases in the percent cover of many other species, including *B. elegans* from 2.9% ± 3.69% between 1969-1974 to 0.94% ± 1.07% between 2008-2011 (Elahi et al. 2013).

To analyze the significance of this change we need to know about *Balanophyllia elegans*' competitors and facilitators and their physical response when these species are present. Coyer and colleagues (1993) studied the effect of sea urchin presence on the abundance of the orange cup coral in California. Sea urchins eat macroalgae, which affect *B. elegans* negatively in various ways. Algal holdfasts compete with *B. elegans* for space and can overgrow them (Coyer et al. 1993) and the fronds also have a harmful effect. When the fronds brush the coral it causes the polyps to withdraw for an extent of time that may allow other species, such as coralline algae, to overgrow them (Coyer et al. 1993). When sea urchins are present they eat macroalgae, decreasing its density and facilitating *B. elegans* survival (Coyer et al. 1993). However, *B. elegans* is not defenseless. In a study at Shady Cove and Turn Island in the San Juan Islands, Bruno et al. (1996) found that *B. elegans* uses aggressive behavior through tentacle contact to ward off competitors. However, as larvae they are susceptible to predation by adult *Corynactis californica* (Chadwick 1991). *C. californica* negatively affects the survival rates of *B. elegans'* larvae, which directly affects their population size since their larvae travel very short distances from the parent polyps (Chadwick 1991).

Abiotic factors, such as flow rate, are also important predictors for *Balanophyllia elegans*' size and distribution (Connel 1961). Flow rate affects coral growth: Schutter et al. studied the hard coral *Galaxea fascicularis* for biomass dependence on flow rates, finding that these corals did better at higher rates. This result is probably due to the higher flow preventing macroalgae growth, removing oxygen radicals and derivatives, and supplying more frequent food (Schutter 2010).

In our research we looked for predictors of *Balanophyllia elegans*' distribution, biomass, and oral disc surface area by analyzing four years of vertical rock wall photos at different depths, sites, and years and modeling biomass accumulation with CHN analyses. We found that all three variables (depth, site, and year) and the interaction variables 'site + depth' and 'site + year + depth' are statistically significant predictors for coral distribution, and year, depth, and the

interaction term ‘year + site’ are significant predictors for oral disc surface area. We still need to analyze our flow and biomass data.

METHODS

Photo Analysis

We analyzed vertical aspect quadrat photos from transects at 11 sites in the San Juan Islands: White Sign, Director’s House, Frost Island, Humphrey Head, Madrona Tree, Pump House, Reid Rock, Rosario Wall, Three Toes, Turn Island, and Willow Island (Table 1; Figure 1). The photos were collected from quadrats along randomly placed 10 m transects on subtidal rock walls at designated sites (Elahi et al. unpublished).

Site	Latitude	Longitude
White Sign	48° 33' 7.959" N	123° 0' 21.658" W
Director's House	48° 32' 48.886" N	123° 0' 25.520" W
Frost Island	48° 32' 25.616" N	122° 50' 35.225" W
Humphrey Head	48° 33' 53.183" N	122° 52' 11.805" W
Madrona Tree	48° 33' 11.386" N	123° 0' 25.210" W
Pump House	48° 32' 45.820" N	123° 0' 27.450" W
Reid Rock	48° 32' 55.852" N	122° 59' 31.704" W
Rosario Wall	48° 38' 36.628" N	122° 52' 25.669" W
Three Toes	48° 32' 58.960" N	123° 0' 20.498" W
Turn Island	48° 32' 2.702" N	122° 58' 9.577" W
Willow Island	48° 32' 25.130" N	122° 49' 24.758" W

Table 1. Site coordinates.

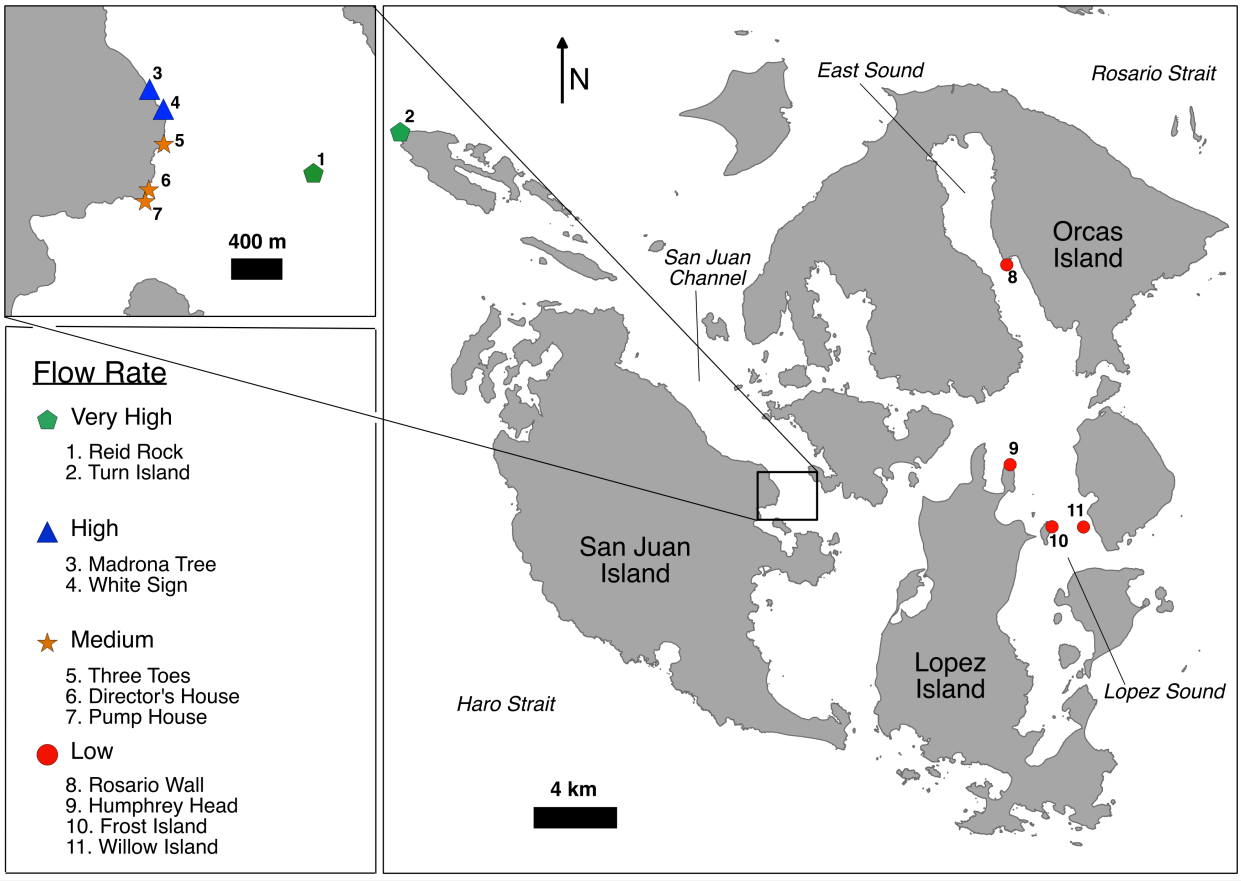

Figure 1. A map of the sites we used during our study.

Photos from two high flow sites, White Sign and Madrona Tree, from the years 2008-2011, were used to quantify *Balanophyllia elegans*' abundance and size at depths ranging from 3 m to 27.5 m with 3 m increments. During the photo analysis, we recorded photos with the presence and absence of *B. elegans*. When we did find a photo that had at least one *B. elegans* in it, we cropped the photo in Preview to restrict the image to the inside of the camera frame, then used ImageJ to set the scale of the image for measurements. We then typed a number next to each coral for reference, traced them, and recorded two diameter measurements from each coral. The photos that didn't have corals were recorded as well, but were not used in biomass calculations.

We analyzed the photos from 2008 slightly differently. In the years before 2009, mobile fauna, such as sea urchins, were not removed from the quadrats before the photos were taken. Therefore, many of the photos from 2008 had large mobile fauna that could possibly be blocking corals, so we didn't analyze those ones.

During our study we also researched the effect of varying flow environments on *Balanophyllia elegans*' size and abundance. We obtained flow data from Elahi and colleagues (unpublished) at the 11 sites between a depth range of 15 m to 21 m with flow rank categories: very high, high, medium, and low flow. The photos were from years between 2008-2013. The flow measurements were obtained by placing alabaster dissolutions blocks at these sites and monitoring them to measure the rate they dissolved. Over this range of flow ranks we analyzed photos for *B. elegans'* size and abundance. All of the corals were counted and recorded per quadrat, but only the 10 largest corals per transect were traced, numbered, and recorded.

Biomass Analysis

Hellstrom et al. studied soft bodied, colonial corals and found a correlation between the disc diameter of a coral and colonial volume (Hellstrom et al. 2011). To resolve *Balanophyllia elegans'* biomass from our photos we made a model from measured coral diameters and the nitrogen content of the respective corals.

Before collecting coral samples, we needed to know if we could accurately measure tissue biomass separate from the skeleton. Koshcheeva et al. (2010) studied methods for optimal CHN analysis results. They found that there are ideal calibration ranges, temperatures, and sequence of steps in CHN analysis to get the most accurate results (Koshcheeva et al. 2010). We used CHN analysis to determine Carbon and Nitrogen content of our samples. We first used a White-Plume Sea Anemone (*Metridium giganteum*) because it doesn't have a skeleton. This morphological characteristic gave us the ability to start with a pure tissue sample and then add increasing amounts of calcium carbonate ($CaCO_3$).

After we collected the sea anemone, we blended it to make it dry faster, and then baked it at temperatures between 60°-70°C for four days, grinding and weighing it often, to make sure we had an accurate tissue mass. Once the mass measurements were consistent, we separated the sample into 11 approximately equal samples and added increasing amounts of $CaCO_3$ to ten of the samples to get ratios of $CaCO_3$ ranging from 1:1 to 1:10. One of the samples was pure tissue so we would know what the nitrogen content of all the samples should be. The results showed that the nitrogen was being partially masked by the $CaCO_3$; we corrected for this in our model.

Due to two odd sample results, we prepared two new replacement samples in the same way, except they were baked for two days before the mass measurements were consistent.

We then sampled ten corals over a range of sizes. Live corals were selected, photographed, and measured by diameter and height, then baked in the oven between 60°-70°C to dry. After one day baking, the corals were individually ground and put back into the oven. These samples were weighed for three days before the mass measurements was consistent and then sent off for CHN analysis. A coral skeleton was also analyzed to assess its nitrogen content. We assumed that a negligible amount of nitrogen is in the skeleton and that the C:N in the coral tissue was the same as the C:N of the sea anemone (Sterner and Elser 2002).

Other methods have been used to determine coral tissue biomass. Johannes et al. (1970) used fine streams of freshwater to remove the soft tissue of corals from their hard skeleton. However, this method is not very accurate because not all of the tissue can be removed by this means. Schutter et al. (2010) used a buoyancy method for determining the tissue weight. More tissue makes the coral more buoyant, so by using an equation they estimated the tissues' weight. They also discuss the inaccuracies of other methods, such as estimating tissue weight from surface area, because tissue growth is not proportional to skeleton growth (Schutter et al. 2010). The skeleton grows continuously while the tissue layers have a different pattern of development (Schutter et al. 2010).

Data Analysis

We used Excel to make models for coral biomass vs. surface area, and coral biomass vs. diameter. To look for trends in distribution and size at Madrona Tree and White Sign, we used R to graph density (count/m^2), largest diameter (mm), surface area (mm^2), and biomass (g) against abundance and depth (m), we graphed largest diameter (mm), surface area (mm^2), biomass (g) and year vs. flow rank, and we graphed average biomass and surface area vs. year. At all 11 sites we looked at trends with density and mean surface area (mm^2), vs. flow (rank). We plotted average biomass vs. coral population density at Madrona and White Sign to look for a correlation.

Multiple statistical tests, including Gaussian General Linear Model and Poisson General Linear Model, were used with ANOVA analysis to determine the significance of year, site, depth or interaction terms as predictors for coral distribution and/or size.

RESULTS

There was some masking of the nitrogen in the anemone CHN analysis results, but the data was linear and well described by the equation ($y = 0.9539x - 0.3508$, $R^2 = 0.8803$) (Fig. 2A). The carbon analysis also showed a linear correlation between the actual C% in the sample and the C% that was analyzed ($y = 0.9539x - 0.3508$, $R^2 = 0.8803$) (Fig. 2B). We made models for the coral's largest diameter vs. tissue biomass ($y = 0.0002e0.4974x$, $R^2 = 0.896$), and surface area vs. tissue biomass ($y = 0.001e0.0488x$, $R^2 = 0.8533$) from the *B. elegans* and sea anemone CHN results; both graphs were fitted with a power function (Fig. 3).

A.

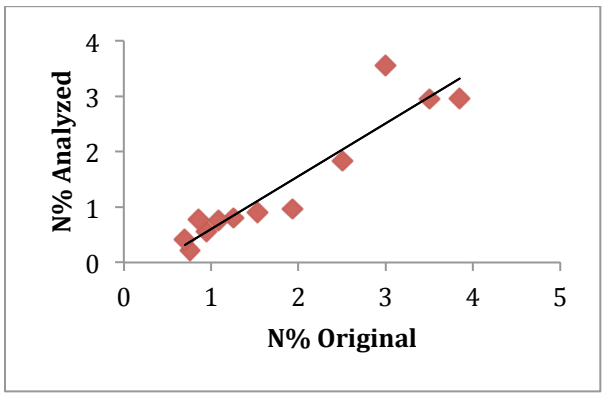

B.

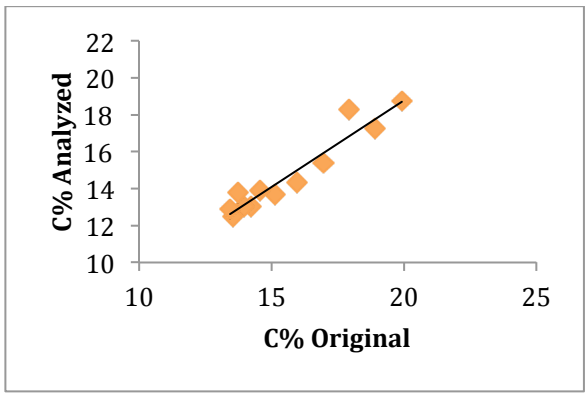

Figure 2. A) The percent nitrogen analyzed by CHN in the anemone samples versus the true percent nitrogen ($y = 0.9539x - 0.3508$, $R^2 = 0.8803$). B) The percent carbon analyzed by CHN in the anemone samples versus the true percent carbon ($y = 0.9379x + 0.0162$, $R^2 = 0.9157$).

A.

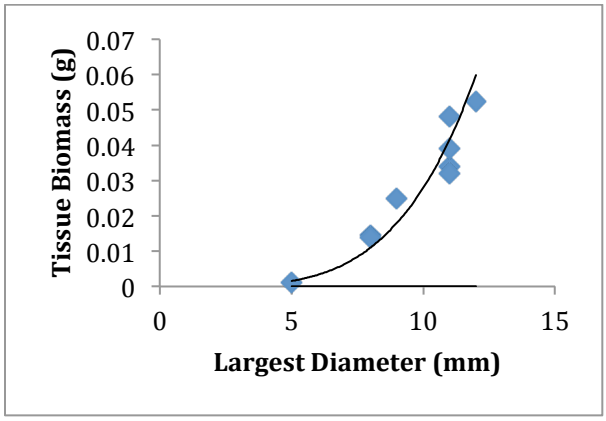

B.

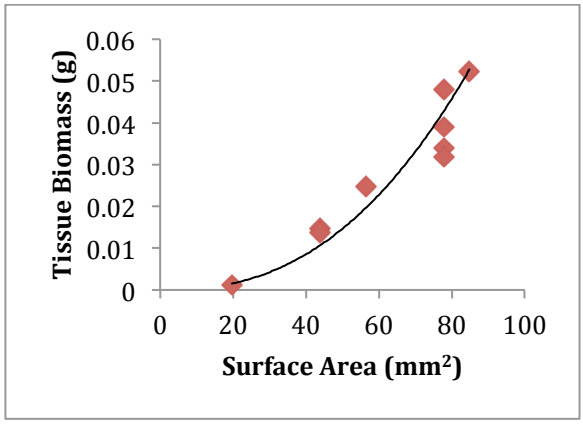

Figure 3. A) The calculated tissue biomass versus the largest diameter for the 10 corals ($y = 2E\text{-}06x^{4.1768}$, $R^2 = 0.9569$). B) The calculated tissue biomass versus the surface area for the 10 corals ($y = 1E\text{-}06x2.4238$, $R^2 = 0.9595$).

We made graphs then ran three models and ANOVA analyses on the combined data from 2008-2011 White Sign and Madrona Tree photos with depths ranging from 3 m to 27 m and the 2008-2013 data from the 11 flow sites with depths between 15 m and 21 m. Our results show that there are different coral distributions at White Sign and Madrona Tree. At White Sign the coral density had two peaks at 9 m and 24 m, where as Madrona Tree had lower overall coral densities, with no corals at 3 m and 6 m and lows at 15 m and 24 m, but had a significant peak in coral density at 21 m (Fig. 4; Fig. 5). Across depth, the largest corals at White Sign are found at 6 m and 18 m and at Madrona Tree they are found at 9 and 15 m (Appendix A; Appendix B).

There are few data points at 3 m and 6 m for sizes because there was not many vertical rock wall photos with corals in them and the ones that were present were to angled to measure

accurately (Appendix C; Appendix D). There are no statistically significant differences in years with the variables average surface area and biomass.

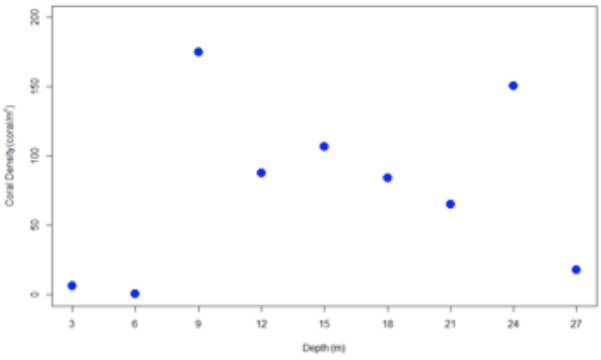

Figure 4. The coral population density (number of corals/m^2) at each depth at White Sign.

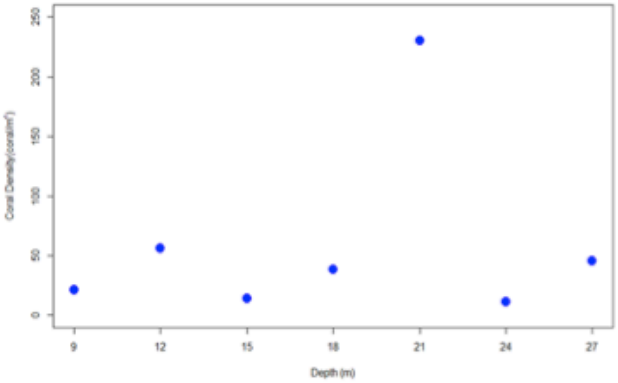

Figure 5. The coral density (number of corals/m^2) at each depth at Madrona Tree.

Highest coral population density is found at high flow sites and the highest biomass is found at very high flow sites (Appendix H). We graphed coral population density and average but we did not find a correlation between density and biomass (Appendix I).

The abundances of largest diameter and surface area at Madrona Tree and White Sign have relatively normal distributions (Appendix F; Appendix G). The distribution of biomass is more of Poisson distribution (Appendix F; Appendix G). At each depth and site, the abundances of largest diameter and surface are still normally distributed, and the biomass has a Poisson curve (Appendix E).

The Poisson General Linear Model was our first model, with the predictors site, depth, and year, and abundance as a response variable. From the ANOVA analysis of this models results we found that all three predictors, site, depth, and year, and two interaction terms 'site + depth' and 'site + year + depth,' were statistically significant predictors for the response variable: coral abundance (Table 2).

Factor	P-Value
Year	$p < 0.001$
Site	$p < 0.001$
Depth	$p < 0.001$
Site * Depth	$p < 0.001$
Site * Year * Depth	$p < 0.001$

Table 2. Significance values of the Poisson general linear model on the coral abundances.

Factor	P-Value
Site	$p < 0.001$
Year	$p < 0.001$
Depth	$p < 0.001$
Site * Year	$p < 0.001$

Table 3. Significance values of the Gaussian general linear model on the individual coral surface areas.

To find predictors for average coral surface area per transect, we used a Gaussian General Linear Model with the predictors site, depth, and year and with average coral surface area as the response variable. When ANOVA was run on this model's results, the only significant predictor was year. We ran this model again, but exchanged the response variable, average coral

surface area per transect, with the individual coral surface areas. The ANOVA analysis on this model showed many more statistically significant predictors: site ($p = 3.650e-09$), year ($p = 9.279e-10$), depth and 'year + site' (Table 3).

DISCUSSION

Our models show an approximately linear increase in oral disc size, but an increasing rate of growth for tissue biomass. We fitted power functions to the two graphs, because you would expect to see this trend given non-linear coral development patterns (Schutter 2010). The model isn't completely accurate, because our C:N results from the CHN analysis have error that may be due to incomplete mixing of our samples. However, the trend is good enough that we can still use our results to get a picture of biomass across depths, sites, and years. However, this analysis will need to be redone. Another part of the equation that needs to be fixed is the correction factor for the amount of N masked by $CaCO_3$. We assumed that the amount of N in the corals would be progressively masked by $CaCO_3$ with increasing coral size, but we weren't accounting for the fact that the C:N in the corals isn't changing as drastically with size as the C:N of the sea anemone samples with added $CaCO_3$.

Our linear models and ANOVA results highlight that the sites, depths, and years are very important predictors for coral abundance and size, and not often can one of these variables alone accurately predict size and distribution, given the interaction terms. Although White Sign and Madrona Tree are near each other and they both have high flow rates, it is not surprising that site is a statistically significant predictor for coral abundance. Fraschettie et al. (2005) found that large variability is common at smaller scales due to many abiotic and biotic factors (Connell 1961). Sedimentation and flow effects on transport of particulate food are highly variable and affect coral mortality (Lesser et al. 1994). Additionally, Gerrodette (1981) proposed that there must be stochastic events spreading *Balanophyllia elegans* due to the observation that in laboratory experiments, their larvae don't crawl much farther than 130 cm from the parent coral before settling (Gerrodette 1981). It is possible that chance events, such as local turbulence, have led to the coral distributions we see at each site.

Depth as a predictor for coral abundance also makes sense. Depth ranges of the corals' food resources, varying flow rates, and predator and competitor ranges can all influence where higher numbers of corals are found. Kelp often limits coral growth when present because the fronds negatively affect their feeding behavior, and the holdfasts compete for space (Coyer et al. 1993). Other organisms that compete for space or brush coral will have a similar negative effect on corals. This is probably why there are no corals in the transect photos from Turn Island at 21 m; the Hydroids are dense in all of these photos. Sea urchins, which feed on kelp, can limit the growth of kelp thereby allowing corals to grow at higher depths they are not often seen at (Miller 1996). Perhaps this is why at White Sign we found the highest densities of corals at 9 m and 24 m, but at Madrona Tree the highest density was at 21 m.

The result that time (year) is a significant predictor also fits with previous *Balanophyllia elegans* research. Without some other force moving *B. elegans* from the parent coral, this species would only extend its range by 7.5 cm/yr (Gerrodette 1981). Also, these corals are estimated to live between 6-40 yrs (Bruno and Witman 1996). Given this information, it's possible that once a

coral population has started at a site it will continue to grow as long as resources, such as food and space, aren't limited. The data we collected show a positive correlation between abundance and year. Since we found that time is a significant predictor, this means we may not be able to aggregate our data across years into one data set to increase sample size. We also only analyzed four years of photos. This is a small sample of years and the first year of photos, 2008, has a slightly different sampling method. In 2008, mobile fauna weren't removed from the quadrat photos, but they were in all future years. Since there weren't many vertical rock well photos from 2008 anyways, the photos we did analyze might not be truly representative of the population. Some of these photos could still be used in this research if we find the area non-covered surface area of the quadrat, then analyze that area, and use the new area measurement in density calculations. We would need to do more years of photo analysis to potentially reduce the significance of small changes between years and changes in sampling method.

The Gaussian General Linear Model for average coral surface showed that "year" was the only statistically significant predictor of size. This could be based on growth over the years of the study. Previous studies have observed that *Balanophyllia elegans* is on average 10 mm in diameter (Bruno and Witman 1996). The corals we found in photos at White Sign and Madrona were most commonly 7-8 mm. This could be a young population that is still growing, supported by the positive trend in abundance over the years of photos and increasing surface area. However, when this model was run again with individual coral surface areas, there were more predictors found. It's possible that points were given more weight because they were averages of the transects, but they did not necessarily have as high of a sample size as other transects. These results tell us that these sites are unique, but each site has an interesting pattern that will need to be defined through further analysis.

The flow analysis found the highest population densities of corals at high flow rank sites and the highest biomass at the very high flow rank sites, but the correlation of these two variables is not significant. One possibility is that higher flow sites support higher population densities due to increased food transport (Lesser et al. 1994) and preferred temperatures (Connel 1961), but at very high flow sites there could be less recruitment in the area because the larvae are being swept away by the current (Roughgarden et al. 1988).

This research is preliminary and there are errors that need to be fixed, but we established a baseline survey of *Balanophyllia elegans'* population characteristics in the San Juan Archipelago that can be used in further research comparing our findings to historical data and in future research to give us a better understanding of how this coral's population is changing.

ACKNOWLEDGEMENTS: Thanks to our advisors Kenneth Sebens and Kevin Turner for their support and years of research; to Robin Elahi for sharing previous research and for long distance support of our project; to Derek Smith, Heather Denham, Jessica Nordstrom, and Tim Dwyer for their work collecting and analyzing data; to the Analytical Service Center at the University of Washington who ran our CHN analyses; to the University of Washington Friday Harbor Labs for providing the tools and resources for us to analyze data; and thanks as well to the Mary Gates Endowment Scholarship for providing financial support.

LITERATURE CITED

Altieri, A. H. (2003) Settlement cues in the locally dispersing temperate cup coral Balanophyllia elegans. *Biological Bulletin*, Vol. 204, pp. 241-246.

Bruno, J.F. and Witman J.D. (1996) Defense mechanisms of scleractinian cup corals against overgrowth by colonial invertebrates. *J. Exp. Mar. Biol. Ecol.*, Vol. 207, pp. 229-241.

Chadwick, N.E. (1991) Spatial distribution and the effects of competition on some temperate Scleractinia and Corallimorpharia. *Mar. Ecol. Prog. Ser.*, Vol. 70, pp. 39-48.

Connell JH (1961) Effects of competition, predation by Thais lapillus, and other factors on natural populations of the barnacle Balanus balanoides. *Ecol. Monogr.* Vol. 31, pp. 61-104

Coyer, J.A., Ambrose, R.F., Engle, J.M. and Carroll J.C. (1993) Interactions between corals and algae on temperate zone rocky reef: mediation by sea urchins. *J. Exp. Mar. Biol. Ecol.*, Vol. 167, pp. 21-37.

Elahi, R., Birkeland, C., Sebens, K.P., Turner, K.R. and Dwyer, T.R. (2013) Limited change in the diversity and structure of subtidal communities over four decades. *Marine Biology*, pp. 1-11.

Elahi, R., Sebens, K.P., and Dwyer, T.R. (Unpublished) Mesoscale variability in oceanographic retention sets the abiotic stage for subtidal benthic diversity. *Unpublished,* pp. 1-58.

Fadlallah, Y.H. (1983) Population dynamics and life history of a solitary coral, *Balanophyllia elegans*, from Central California. *Oecologia*, Vol. 58, pp. 200-207.

Fraschetti S., Terlizzi A., Benedetti-Cecchi L. (2005) Patterns of distribution of marine assemblages from rocky shores: evidence of relevant scales of variation. *Mar. Ecol. Prog. Ser.* Vol. 296, pp. 13-29

Gerrodette, T. (1981) Dispersal of the solitary coral *Balanophyllia elegans* by demersal planular larvae. *Ecology*, Vol. 62, pp. 611-619.

Hellstrom, M. (2011) Robustness of size measurement in soft corals. *Coral Reefs*, Vol. 30, pp. 787-790.

Johannes, R.E. (1970) Method for determination of coral tissue biomass and composition. *Limnology and Oceanography*, Vol. 15(5) pp. 822-823.

Koshcheeva, O.S., Zubareva, A.P. and Saprykin, A.I. (2010) CHN analysis of functional materials and their precursors. *J. Structural Chem.*, Vol. 51, pp. 175-178.

Lesser MP, Witman JD, Sebens KP (1994) Effects of flow and seston availability on scope for growth of benthic suspension-feeding invertebrates from the Gulf of Maine. *Biol. Bull.* Vol. 187, pp. 319-335

Maier-Reimer, E. and Hasselmann, K. (1987) *Transport and storage of CO2 in the ocean: An inorganic ocean-circulation carbon cycle model. Climate Dynamics*, Vol. 2:2, pp. 63-90.

Microsoft (2011) Microsoft Excel [computer software]. Redmond, Washington: Microsoft.

Miller, M.W. and Hay, M.E. (1996) Coral-seaweed-grazer-nutrient interactions on temperate reefs. *Ecological Monographs*, Vol. 66:3, pp. 323-344.

Orr, J.C., Fabry, V.J., Aumont, O., Bopp, L., Doney, Scott C., Feely, Richard A., Gnanadesikan, A., Gruber, N., Ishida, A., Joos, F., Key, R.M., Lindsay, K. Maier-Reimer, E., Matear, R., Monfray, P., Mouchet, A., Najjar, R.G., Plattner, G., Rodgers, K.B., Sabine, C.L., Sarmiento, J.L., Schlitzer, R., Slater, R.D., Totterdell, I.J., Weirig, M., Yamanaka, Y., and Yool, A. (2005) Anthropogenic ocean acidification over the twenty-first century and its impact on calcifying organisms. *Nature*, Vol. 437:29, pp. 681-686.

R Core Team (2013) R: A language and environment for statistical computing. R Foundation for Statistical Computing, Vienna, Austria. URL http://www.R-project.org/.

Rasband, W.S. (1997-2012) ImageJ, U. S. National Institutes of Health, Bethesda, Maryland, USA, http://imagej.nih.gov/ij/

Roughgarden J, Gaines S, Possingham H (1988) Recruitment dynamics of complex life cycles. *Science,* Vol. 241, pp. 1460-1466

Schutter, M. (2010) The effect of different flow regimes on the growth and metabolic rates of the scleractinian coral *Galaxea fascicularis*. *Coral Reefs*, Vol. 29, pp. 737-748.

Sterner, R.W. and Elser, J.J. (2002) Ecological Stoichiometry: The Biology of Elements from Molecules to the biosphere. *Princeton University Press.* Print.

Szmant-Froelich, A., Yevich, P., and Pilson M.E.Q. (1980) Gametogenesis and Early Development of the Temperate Coral Astrangia danae (Anthozoa: Scleractinia). *Biological Bulletin*, Vol. 158, pp. 257-269.

APPENDIX

A. B. C.

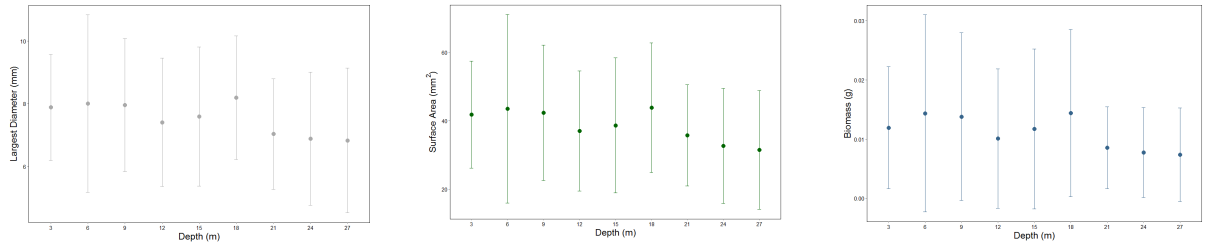

Appendix A. The means and standard deviations of A) largest diameter, B) surface area, and C) biomass over depth at White Sign (n=1147).

A. B. C.

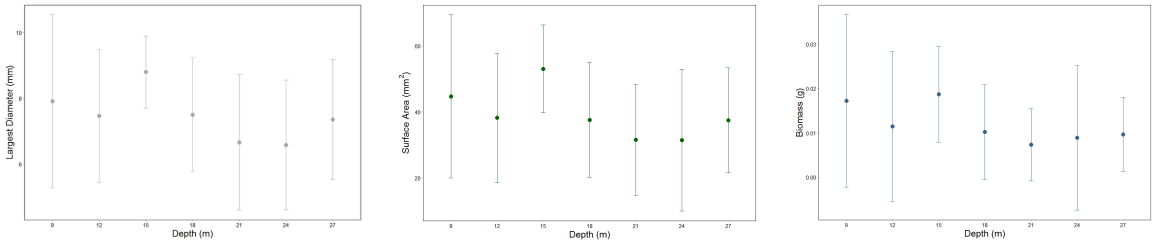

Appendix B. The means and standard deviations of A) largest diameter, B) surface area, and C) biomass over depth at Madrona Tree.

A. B.

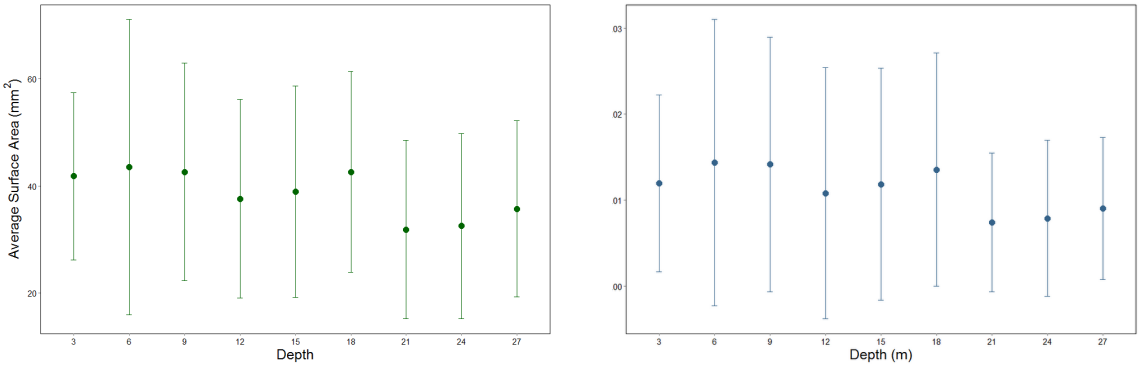

Appendix C. The A) mean coral surface area versus depth and B) average biomass versus depth for both White Sign and Madrona Tree. Each average is calculated over all years.

A.

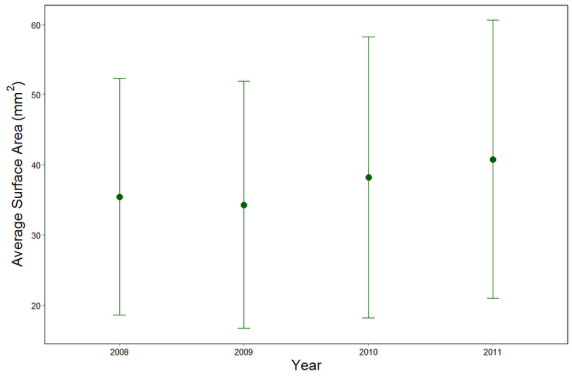

B.

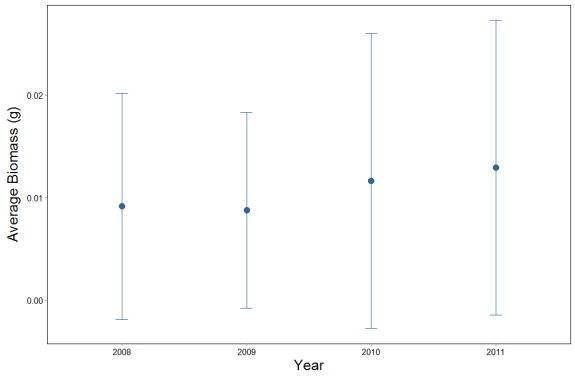

Figure 9. The A) average coral surface area versus year and B) average biomass versus year for White Sign and Madrona. Each average is calculated from a specific, year, site and corresponding depth.

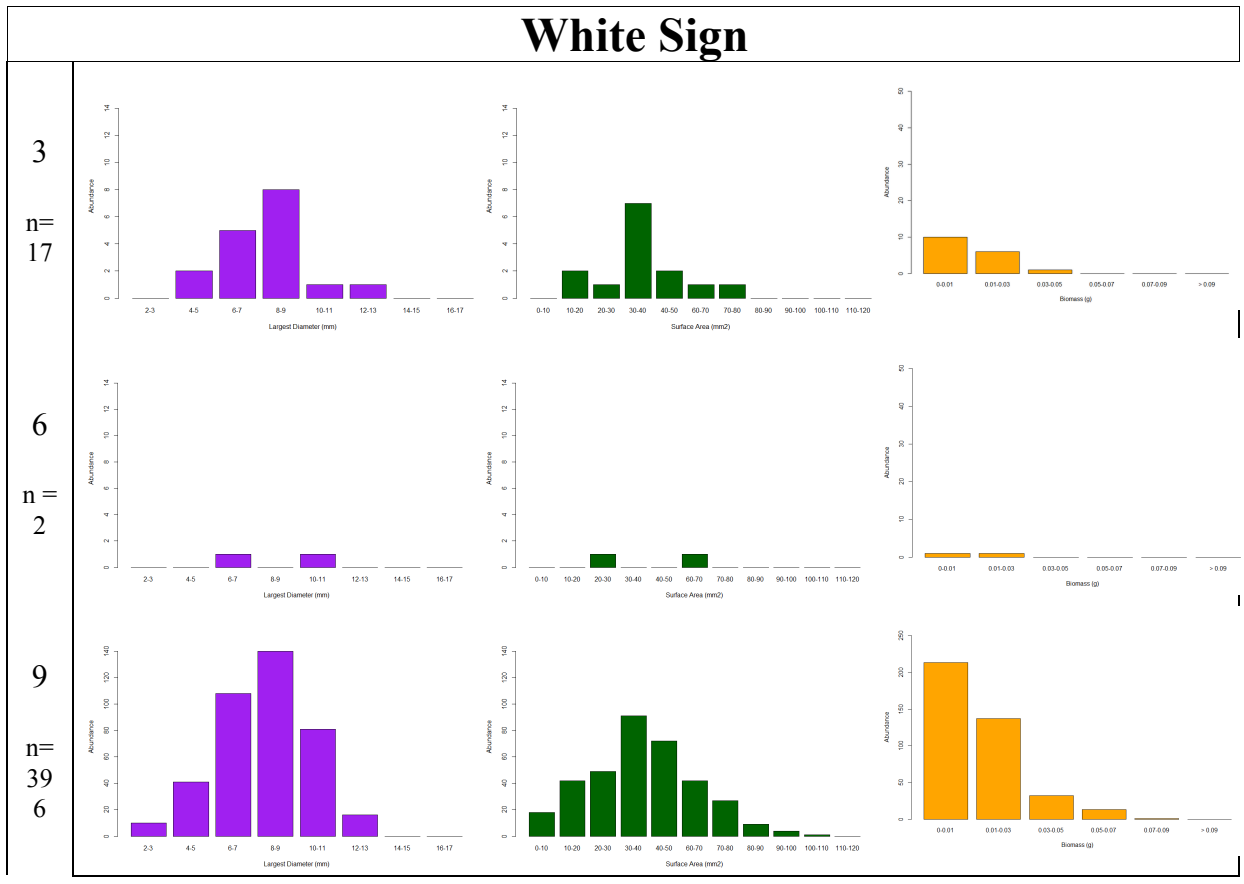

12

n=
187

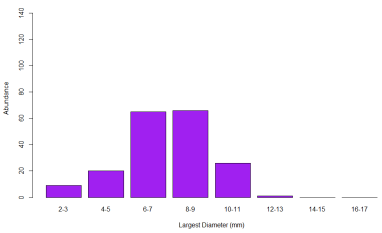

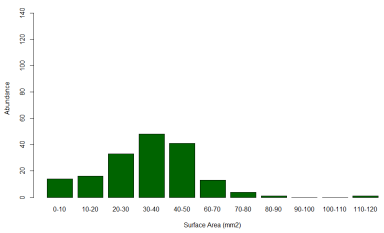

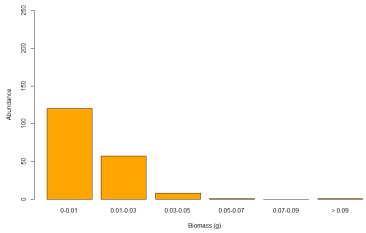

15

n=
290

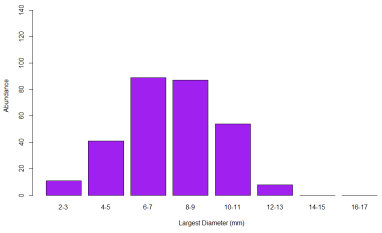

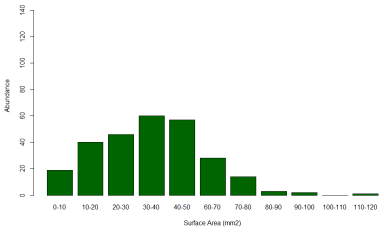

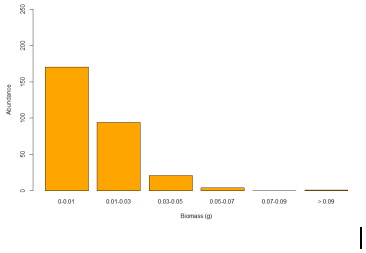

18

n=
110

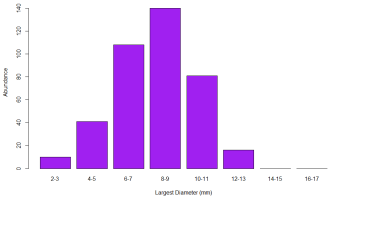

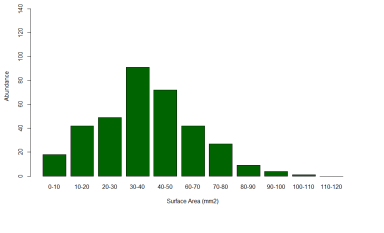

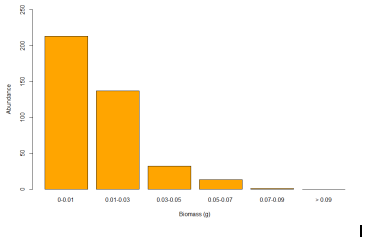

21

n=
29

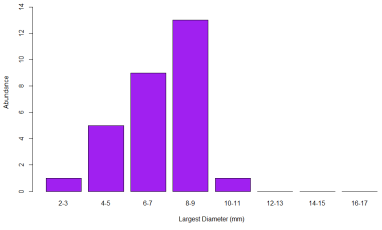

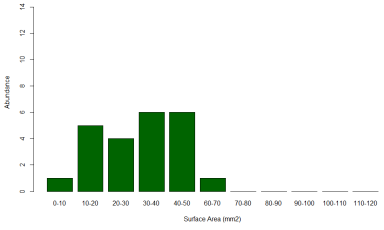

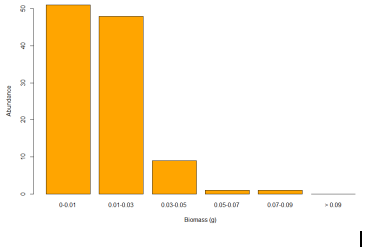

24

n=
81

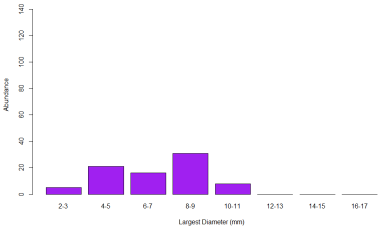

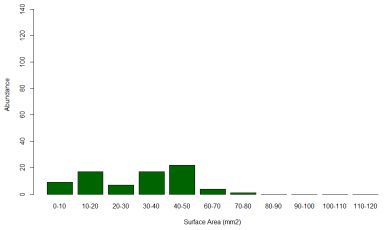

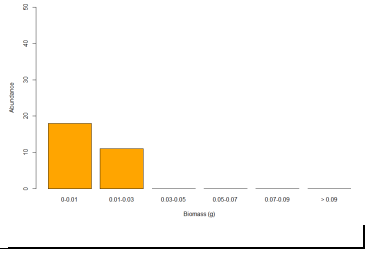

27 n= 35	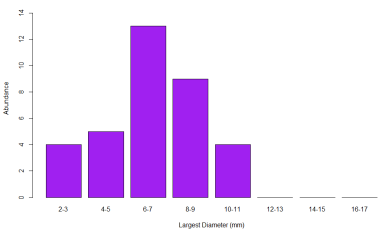	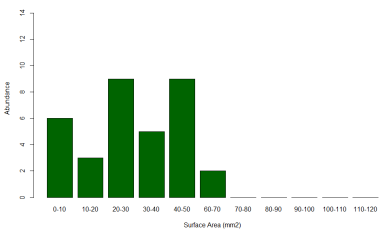	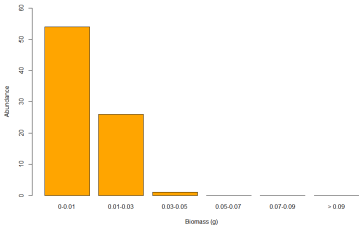

Madrona Tree

9 n= 46	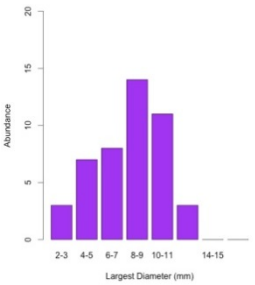	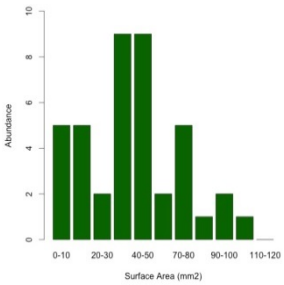	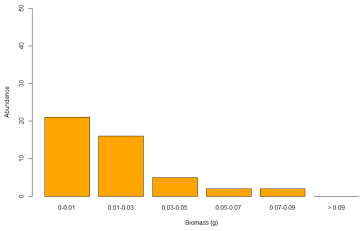
12 n= 19 5	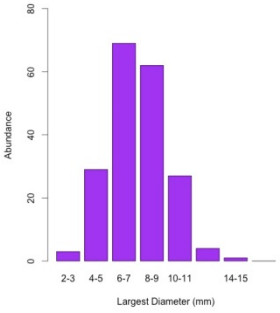	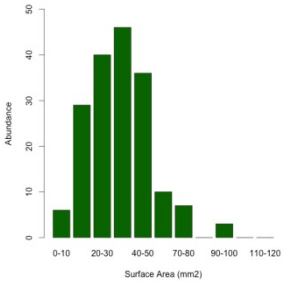	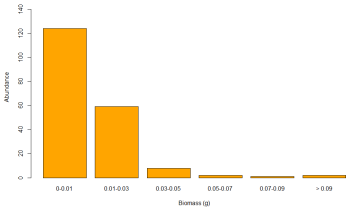
15 n= 5	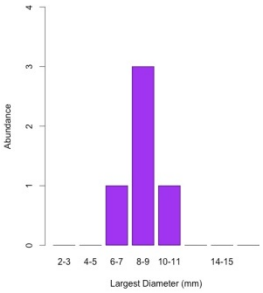	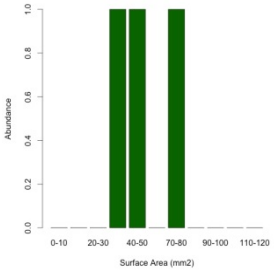	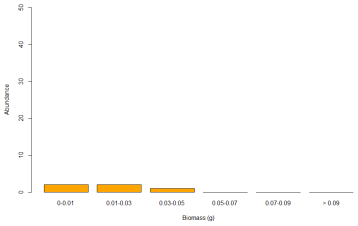
18 n= 28	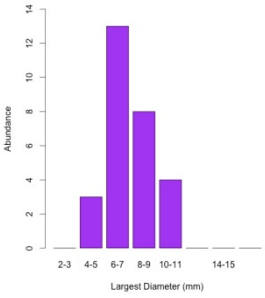	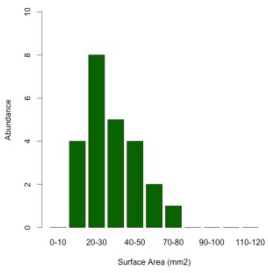	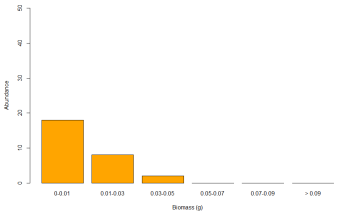

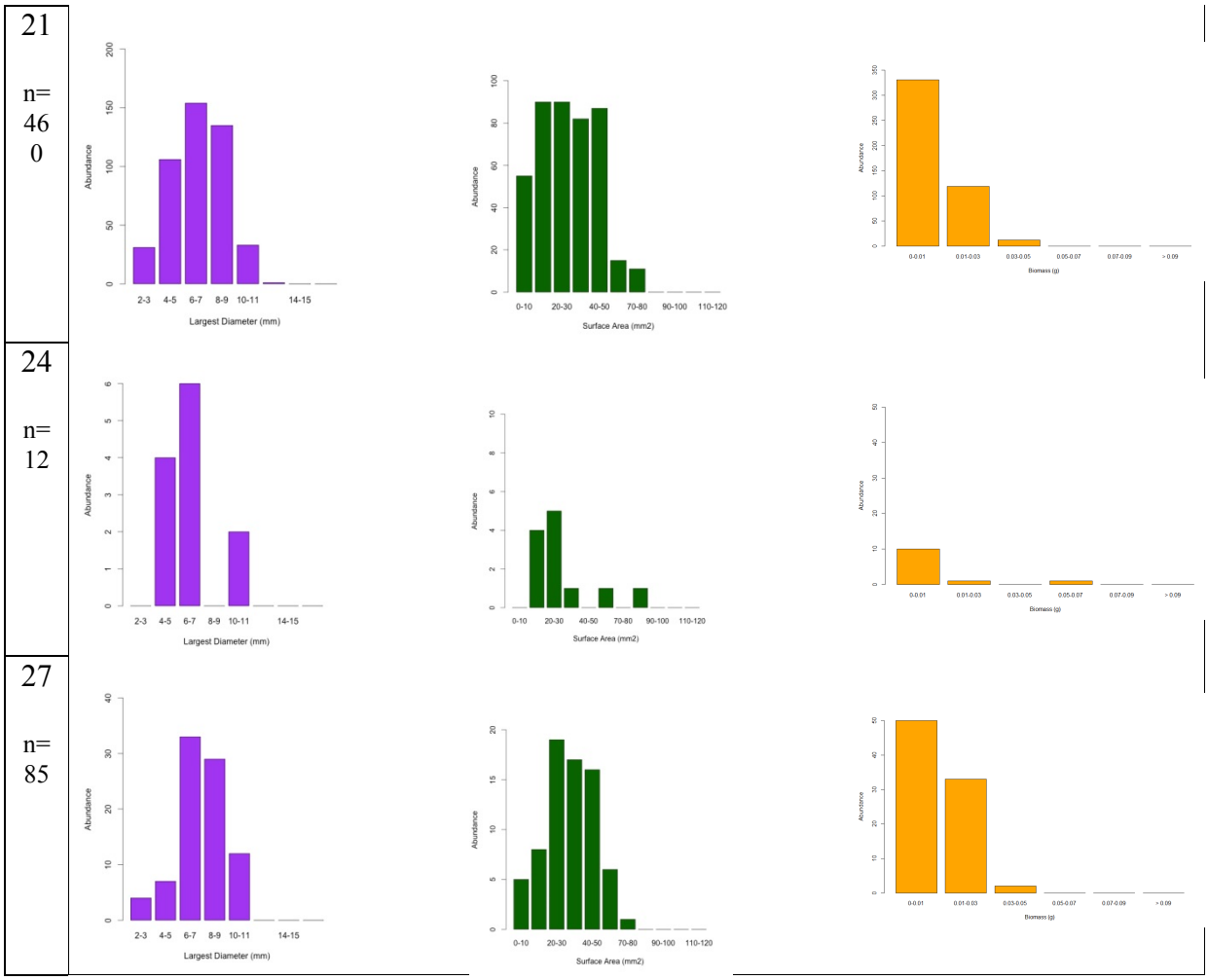

Appendix E. The abundances of largest diameter, surface area and biomass separated by depth at White Sign and Madrona Tree.

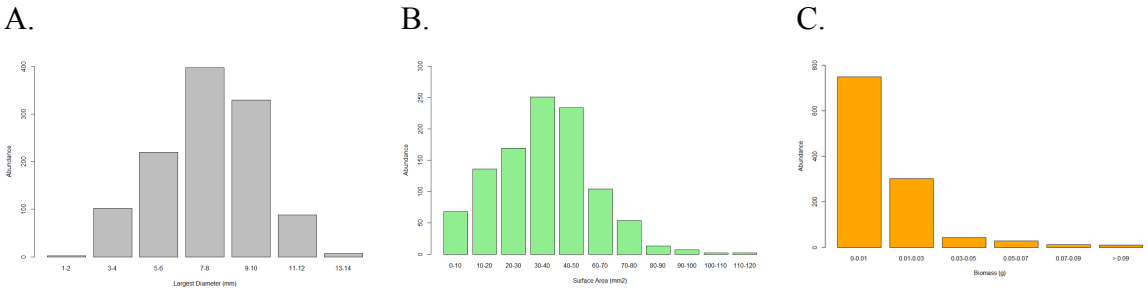

Appendix F. The abundances of A) largest diameter, B) surface area, and C) biomass at White Sign (n = 1147).

A. B. C

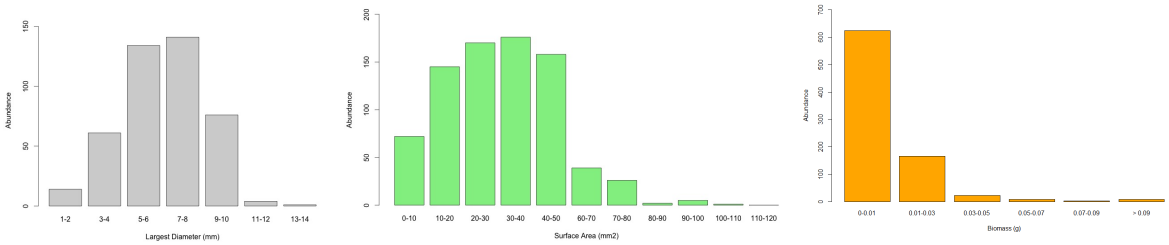

Appendix G. The abundances of A) largest diameter, B) surface area, and C) biomass at Madrona Tree (n = 831).

A. B.

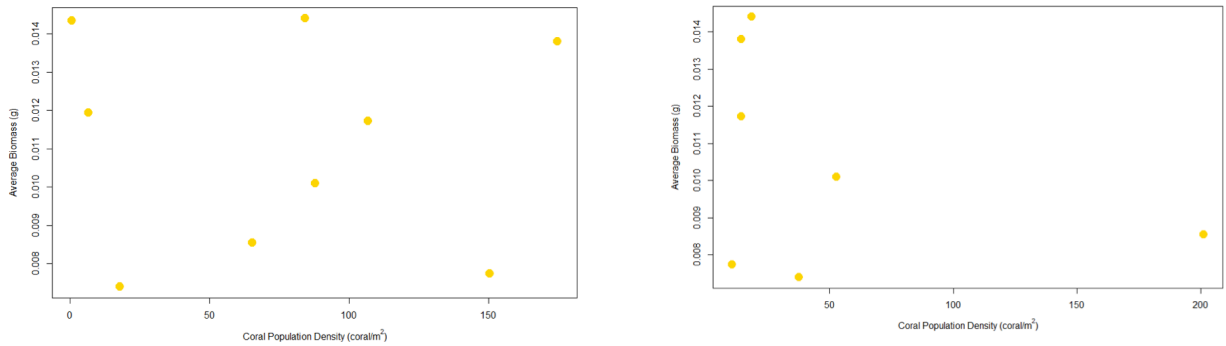

Appendix H. The average biomass plotted against the coral population density at each depth for A) White Sign and B) Madrona. There is no correlation between average biomass and coral population density.

A. B.

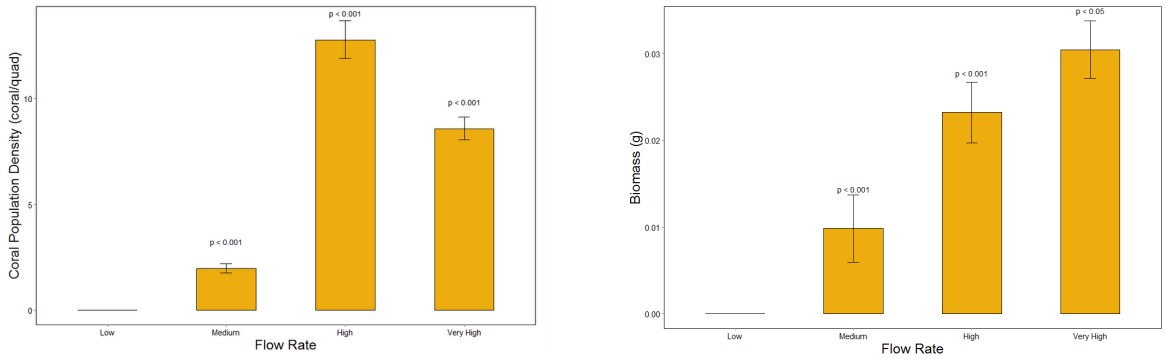

Appendix I. The A) population densities (n=170) and B) average biomasses (n=233) at different flow rates. Highest density does not correspond with highest biomass.